

The Manufacturing Engineering Society International Conference, MESIC 2013

Analysis of the state of stresses and plastic strains during the necking process in ductile steels

Hortigón Fuentes, B.^a, Nieto García, E.J.^a, Herrera Garrido M.A.^{a,*}

^a *Department of Mechanics of Continuous Media, Theory of Structures and Geotechnical Engineering. University of Seville, C/ Virgen de Africa, 7, 41005 Seville, Spain*

Abstract

In steel, the knowledge beyond the yield strength elastic is of the utmost importance because of the large plastic strain that take place both at the time of the breakage and multiple conformation processes involving a stretch of material, such as rolling or extrusion. Beyond the manufacturing process, the trend nowadays is to the use of more ductile steels for concrete every time, that improve the behavior of structures due to loads limits such as those produced by seismic events.

In this investigation, based on breakage testing tensile, we present a detailed analysis of the behavior of ductile steels, manufactured by hot rolling, defining plastic behavior of these laws to breaking, focusing primarily on the phenomenon of the formation of the neck.

© 2013 The Authors. Published by Elsevier Ltd. Open access under [CC BY-NC-ND license](https://creativecommons.org/licenses/by-nc-nd/4.0/).

Selection and peer-review under responsibility of Universidad de Zaragoza, Dpto Ing Diseño y Fabricacion

Keywords: Rolling; plastic flow; ductility; concret bars.

1. Introduction

The stress-strain diagram for investigated steels presents two regions clearly differentiated during the phase of plastic behavior. The first one is bounded between the lower yield point (f_{yi}) and the value of maximum strength (f_u) and it is considered an uniaxial state of stress and a homogeneous strain along the entire length of the specimen. The second one starts when the maximum strength (f_u) value is reached and ends with rupture of the test specimen.

* Corresponding author. Tel.: +34 95 455 28 28; fax:+34 95 455 10 99.

E-mail address: bhortigon@us.es

Necking starts, in which the state of stress becomes triaxial, focusing strain on neck. For this second phase, the stress-strain diagram does not offer information about the behavior of this area; only sample the download status is that submitted the rest of the test specimen.

To know stresses and strains in the first stage, it is necessary to apply to the values of the test equations of Nadai, which is considered the reduction of area suffering section because its elongation, based on the incompressibility of the material and in permanence of the cylindrical geometry.

$$\varepsilon = \frac{L - L_0}{L_0} = \frac{L}{L_0} - 1 = \frac{A_0}{A} - 1 \Rightarrow \frac{A_0}{A} = 1 + \varepsilon \quad (1)$$

$$\sigma_{real} = \frac{F}{A} = \frac{F}{A_0} \cdot \frac{A_0}{A} = \sigma(1 + \varepsilon) \quad (2)$$

Traditionally, the easiest way to define the behavior of materials during this first stage is by the empirical equation of Hollomon

$$\sigma_z = k\varepsilon^n \quad (3)$$

Where n is the strain hardening index, which coincides with strain for maximum actual strength ($\varepsilon_{s\ real}$) and k is force curve to pass through the point of maximum strength ($\sigma_{s\ real} - \varepsilon_{s\ real}$).

For the necking phase, currently still apply models of behavior determined by Davidenkov-Spiridnova (1946) and Bridgman (1952), during the decades of the 1940s and 1950s. Studying the problem since the laws of plasticity, Bridgman initially defined the equations that determine the average axial stress and strain on the minimum section of the neck, based on the hypothesis that the cross section in the necking area remains circular, deformations are constant at all points in this section and the contour of the neck is approaching a circumference arch and, therefore, the lines defining the main tensions have the same geometry.

Bridgman raises valid Hollomon potential equation for this period by applying a corrective factor to mean in the minimum cross-section (σ_z) stress to obtain stress creep (σ_f) of material, according to the plastification of Von Mises criterion, attending to the deformation of the neck at the time of the break.

$$\dot{\varepsilon}_z = -2 \ln \frac{D}{D_0} \quad (4)$$

$$\bar{\sigma}_z = \frac{1}{\pi D^2/4} = \sigma_f \left(1 + \frac{R}{2a}\right) \ln \left(1 + \frac{a}{2R}\right) \quad (5)$$

being,

D_0 the initial diameter of the test specimen, D the instant the minimum section, in equation (5) diameter measured in fracture, R the radius of curvature of the neck fracture and the radius of the minimum section in fracture.

Because of the difficulty involved in measuring the value corresponding to the radius of the arc that forms the shape of the neck during the trial, Bridgman (1952) raised the following relationship between the a/R relationship and real strain $\varepsilon_{z\ real}$:

$$\frac{a}{R} = \sqrt{\varepsilon_{z\ real} - 0'1} \quad \text{Para } \varepsilon_{z\ real} > 0'1 \quad (6)$$

Studies of Kaplan (1973), which determined a relationship $a/z = 0.87$ in fracture for ductile steels, z being the half of the height of the neck area affected by tri-axial tensions exist only regarding the evolution of the geometry of the neck.

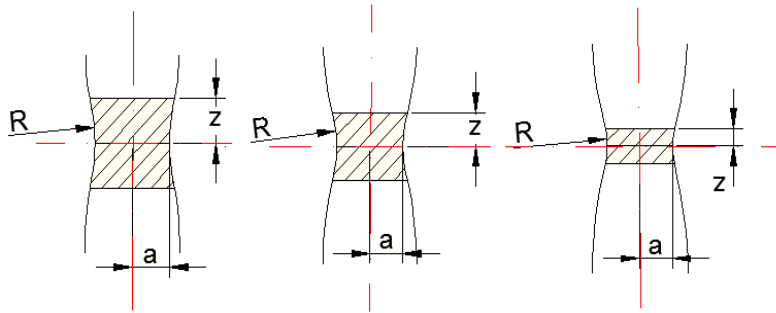


Fig. 1. Evolution of area affected by tri-axial stress at the neck.

This investigation has tried to adjust the curve of plastic behavior of material in both phases. On the one hand, it has parameterized creep curve up to maximum voltage performing an adjustment of the values Hollomon coefficients.

For the necking, are based on the hypothesis that the neck does not deform like a cylinder so it is not valid logarithmic strain used since the 1940s. Through an image processing has been analyzed the evolution of its geometry and real elongation zone determining new curves of the material behavior, taking as the value of uniaxial tension in the minimum cross section $\bar{\sigma}_z = P/A$, where P is the instant strength and A the cross-sectional area of the minimum cross section.

2. Experimental methodology

2.1. Characteristics of material

The characteristics of the material are similar to those of the corrugated steel B500SD, regulated in Spain by EHE-08 (2008) and UNE 36065 (2011), manufactured through a process of hot lamination and later called TEMPCORE controlled cooling process. The steel was supplied by the company Siderurgica Sevillana S.A. In this first phase, 5 cylindrical specimens of smooth steel, length 24' 5mm and diameter of 14 mm have been tested.

Table 1. Mechanical characteristics of the material

f_y	537,80 Mpa
f_{yreal}	541,50 Mpa
f_s	630,80 MPa
f_{sreal}	635,20 Mpa
f_s/f_y	1,17
$\epsilon_{max}(\%)$	12,00
$\epsilon_{u,5}(\%)$	25,65

Table 2. Chemical properties of the material (%)

C	Si	Mn	P	S	Cr	Ni	Mo	V	Cu	Ti	N
0,15	0,16	0,65	0,027	0,04	0,16	0,10	0,02	0,00	0,46	0,00	0,009

The percentage of carbon equivalent is:

$$\%C_{eq} = \%C + \frac{\%Mn}{6} + \frac{\%Cr + \%Mo + \%V}{5} + \frac{\%Ni + \%Cu}{15} = 0'33\%$$

2.2. Test execution

Testing's have been executed in Laboratory of Materials and Structures of the Polytechnic Higher School of the University of Seville, belonging to the Department of Science of Materials and Mechanics of Continuous Media, Theory of Structures and Geotechnical Engineering.

The machine used is the brand "Shimadzu", model AG-X, with a maximum load of 300 kN and an uncertainty of a ± 1 of strength measurement for calibrated range 30 to 300 kN and $\pm 0, 1$ for over 10 mm displacement (confidence level 95% and K=2 coverage factor).

For the determination of the elastic module (E) has been used an extensometer brand MF, model MFA25 with an uncertainty of measurement (level of confidence 95%, K=2):

- For calibration range between 2.5000 mm and 25. 0000mm: 109.9 microns
- For calibration range between 0.2500 mm and 2.5000 mm: 6.1 microns



Fig. 2. Marking of specimens process.

We have worked with a calibrated length of 110 mm, with a marking of specimens each 2.5 mm, using a metal template developed in machining workshop.

The entire process of each test is controlled with the software "TrapeziumX version 1.1. 0b". The test speeds have been $10 \frac{N}{mm^2 \text{ sec}}$ in the elastic stretch, $10 \frac{mm}{min}$ from the elastic limit (f_y) until maximum stress (f_s) and $5 \frac{mm}{min}$ in the necking.

All the tests have been recorded with a video camera "Sony Handycam HDR-XR160E" to 1080 p with resolution 4.2Mpix and 30 x optical zoom. At the same time, has been made a recording of the evolution of the test on the computer with the software "Camtasia 7" screen, allowing you to associate images in the camera rig diagram specific data.

2.3. Treatment of data

Software "TrapeziumX", in addition to the characteristic parameters of the tensile test, gets a table that contains values Strength-displacement every 10 msec, resulting from the 23.000 data order by specimen being tested.

On the other hand, obtained with the camera recording is related to the data table above due to the recording of screen conducted by the program "Camtasia", allowing you to associate images with specific data. Taken 14 frames of each trial, through the program "Sony Vegas Pro 9.0". The first corresponds to the time prior to the trial, and the remaining 13 correspond to the last the time of maximum load moment of the necking.



Fig. 3. Frame one of the specimens during the necking.

The imaging process is carried out in the laboratory of the Department of Materials Science at the Superior Technical School of Engineering.

Each frame is treated with the software "Adobe Photoshop CS4", giving them a resolution of 1 x 1 pixels. Subsequently, is a measurement of the distance between points with "Image-Pro MC" software.

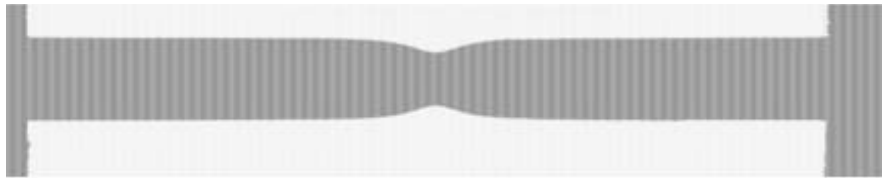


Fig. 4. Frame one of the specimens treated with "Adobe Photoshop CS4".

In this way, are therefore two types of data, the geometric, treatment outcome of frames, which work to analyze the evolution of the geometry of the necking and stresses and strains in this area, and rig data obtained from the test machine, which will be used for the obtaining of tensions to fracture and strains up to the value of maximum strength (f_s).

The numerical data obtained from the frames have been subsequently treated with software "Graph" for the determination of the corresponding curves.

3. Results

3.1. Plastic behavior before necking

Based on the force of each test data were obtained the real stress-strain diagrams and the empirical curves Hollomon, making an adjustment of the latter to the following equation:

$$\sigma_z = \frac{764,708353}{0,1966751^{0,26213109}} \varepsilon_z^{0,26213109}$$

The parameterization of the equation is:

$$\sigma_z = \frac{\sigma_{s_{real}}}{\varepsilon_{s_{real}}^{1,3\varepsilon_{s_{real}}}} \varepsilon_z^{1,3\varepsilon_{s_{real}}} \quad (7)$$

where,

$\sigma_{s_{real}}$, maximum real stress (*)

$\varepsilon_{s_{real}}$, real strain associated with such a stress(*)

(*) Obtained by using the equations of Nadai

Figure 5 shows the three curves, noting the setting of the new equation posed to the curve real stress-strain, with a coefficient of determination $R^2 = 0,988$.

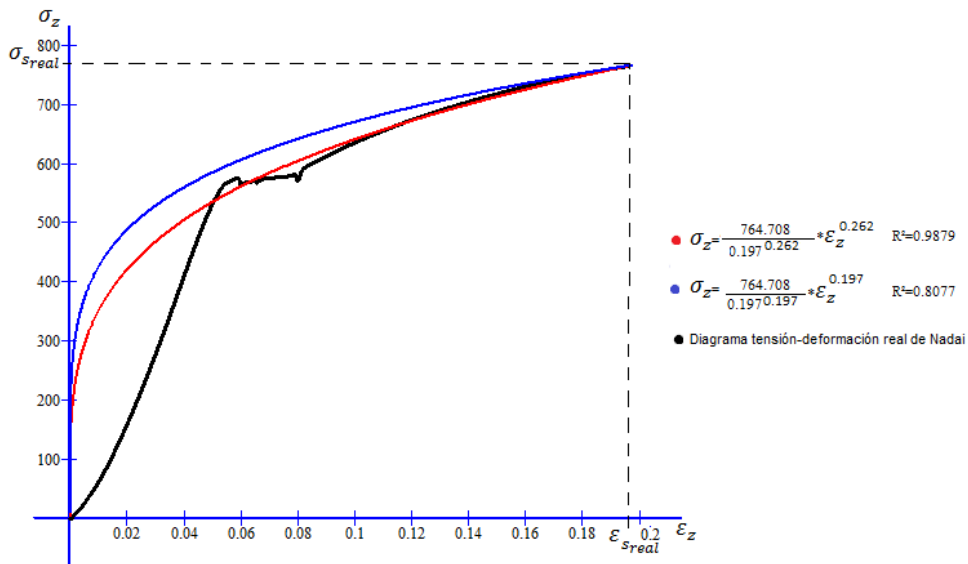


Fig. 5. Plastic behavior up to maximum strength curve. Comparison between the empirical Hollomon curve and the experimental curve.

3.2. Plastic behavior during necking

For the determination of the values of mean minimum section stress has been taken the value F , being F instant strength and A the area of the cross section. Values of strain (ϵ) have been obtained by measuring elongation experienced by the sections affected by the necking, which have bounded from the moment in which begins to see the formation of the neck, and therefore fails to result in a deformation of cylindrical type.



Fig. 6. Measured sections to determine the elongation at necking.

The obtained curve yields results in break of 1171,43 MPa for the mean axial stress and strain of the 54,59%. The law of behaviour of the material is parameterized according to the following equation

$$\sigma = \frac{\sigma_{r\ real} - \sigma_{s\ real}}{(\varepsilon_{r\ real} - \varepsilon_{s\ real})^2} \varepsilon^2 - 2\varepsilon_{s\ real} \frac{\sigma_{r\ real} - \sigma_{s\ real}}{(\varepsilon_{r\ real} - \varepsilon_{s\ real})^2} \varepsilon + \varepsilon_{s\ real}^2 \frac{\sigma_{r\ real} - \sigma_{s\ real}}{(\varepsilon_{r\ real} - \varepsilon_{s\ real})^2} \tag{8}$$

where,

$\sigma_{s\ real}, \varepsilon_{s\ real}$, maximum real stress real strain associated with such a stress(*)

$\sigma_{r\ real}, \varepsilon_{r\ real}$, real axial stress and strain at fracture

(*) Obtained by using the equations of Nadai

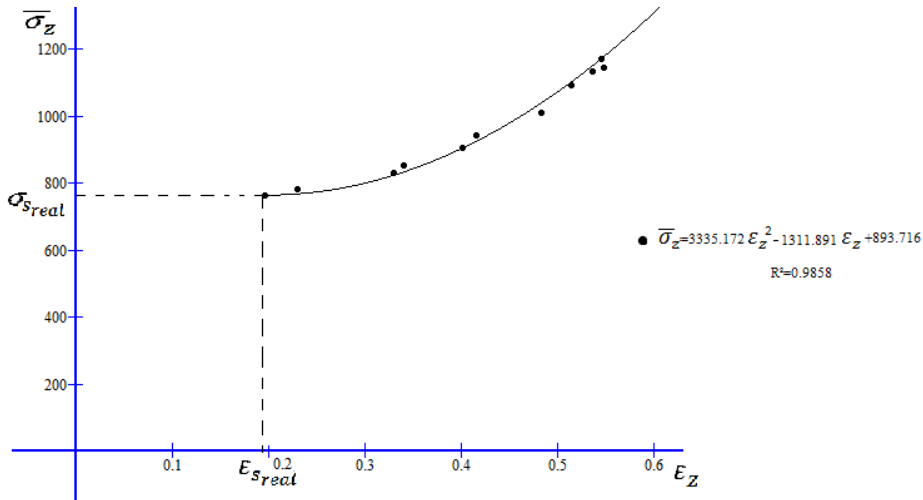


Fig. 7. Law of behavior during the necking σ - ε .

The a/z relationship obtained in break relationship is 0,88, very close to the value obtained by Kaplan (1973) referred to in paragraph 1.

4. Conclusions

The results allow to determine the new laws of plastic behaviour to break for the type of steel studied. These laws are easy to determine to be related with parameters obtained from significant values of the resulting tests Stress-Strain diagram.

Shows that for materials with region of creep, a readjustment of the empirical equation of Hollomon, who is determined to this steel in concrete is necessary.

For behaviour at necking phase law, replacing transverse deformation values traditionally used by those obtained by measuring the elongation real, thus discarding the hypothesis of a cylindrical deformation in the area of the neck.

Our research will continue in the line to extend the study submitted to a total of 30 samples, according to the established in the UNE EN 1080 (2006) and subsequently confirm the results by using the FEM method.

References

Bridgman, P.W., 1952. Studies in Large Plastic Flow and Fracture. McGraw-Hill, London.
 Davidenkov, N.N., Spiridnova, N.I., 1946. Mechanical Methods of Testing. Proceedings of the American Society for Testing and Materials 40, 1147-1158.

García, C., Gabladón, F., Goicolea, J.M., Mirasso, A., Raichman, S., 2004.. Simulación Computacional del Ensayo de Tracción Simple con Estricción. Proyect PICT 12-03268, Spain.

Instrucción de Hormigón Estructural EHE-08. Real Decreto 1247/2008 de 18 de Julio. Spain.

Kaplan, M.A., March 1973. The Stress and Deformation in Mild Steel During Axisymmetric Necking. *Journal of Applied Mechanics*, 271–276.

UNE 36065:2011: Barras corrugadas de acero soldable con características especiales de ductilidad para armaduras de hormigón armado.

AENOR Ediciones, Madrid.

UNE-EN 10080:2006: Acero para el armado del hormigón. Acero soldable para armaduras de hormigón armado. Generalidades. AENOR Ediciones, Madrid.